Journal of Materials Chemistry A

Accepted Manuscript

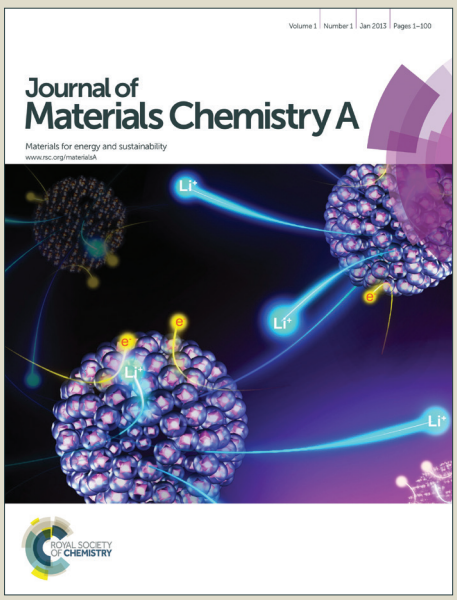

ROYAL SOCIETY OF CHEMISTRY

www.rsc.org/materialsA

Journal Name

RSCPublishing

ARTICLE

Measuring oxygen surface exchange kinetics on mixed-conducting composites by electrical conductivity relaxation

Cite this: DOI: 10.1039/x0xx00000x

Received 00th January 2012,
Accepted 00th January 2012

DOI: 10.1039/x0xx00000x

www.rsc.org/

Bobing Hu,[a] Yunlong Wang,[a] Zhuoying Zhu,[a] Changrong Xia,[*a] Henny J. M. Bouwmeester[*a,b]

The oxygen release kinetics of mixed-conducting $Sr_2Fe_{1.5}Mo_{0.5}O_{6-\delta}$ – $Sm_{0.2}Ce_{0.8}O_{2-\delta}$ (SFM-SDC) dual-phase composites has been investigated, at 750 ^oC, as a function of the SDC phase volume fraction using electrical conductivity relaxation (ECR) under reducing atmospheres, extending our previous work on the oxygen incorporation kinetics of these composites under oxidizing conditions. Gas mixtures of H_2/H_2O and CO/CO_2 were used to control step changes in the oxygen partial pressure (pO_2) in the range 10^{-24} – 10^{-20} atm. At the conditions of the experiments, oxygen re-equilibration is entirely controlled by the surface exchange kinetics. A model is developed which allows deconvolution of the effective time constant of the relaxation process in terms of the intrinsic contributions of the components to oxygen surface exchange and synergetic contributions caused by heterogeneous interfaces. The oxygen surface exchange kinetics under H_2/H_2O atmosphere is found to be a weighted average of the intrinsic contributions of SFM and SDC phases. No evidence is found for an enhanced exchange rate at the SFM-SDC-gas triple phase boundaries (TPB). Synergetic contributions arise under CO/CO_2 atmosphere, enhancing the rate of oxygen surface exchange up to a factor of 2.4. The obtained results are discussed in terms of the surface microstructure of the composites from image analysis. Overall, the results of this and our previous study confirm that the triple phase boundaries in SFM-SDC composites significantly accelerate the oxygen incorporation kinetics under oxidizing conditions, but only modestly, or even negligibly, influence the oxygen release kinetics under reducing conditions.

Introduction

Dual-phase composites consisting of a purely ionic conducting oxide and an electronic - or mixed ionic-electronic – conducting phase are presently being investigated for use as oxygen separation membrane.[1,2] Possible applications include integration in oxyfuel combustion power generation with CO_2 capture,[3-5] and use in membrane reactors for conversion of natural gas to syngas[6,7] or oxidative dehydrogenation of light alkanes.[8,9] The difficulty in identifying single-phase mixed-conducting membranes with high thermochemical stability and durability under both oxidizing and reducing conditions, humid and/or CO_2-containing atmospheres as required in the targeted applications has indirectly stimulated the research in composite membranes. The investigations run parallel with those in the field of solid oxide fuel cells (SOFCs), where such composite materials are aimed for use as electrodes to extend the amount of active triple phase boundaries (TPB).[10,11] An increase of length per unit area of electrode increases the number density of catalytically active sites, and therefore fuel cell performance. Contrary to the electrode, which must be porous to allow gaseous species to diffuse to, and from, the reaction sites, the composite membrane is sintered to full density to avoid unwanted leakage. The functional properties of the membrane can be tailored by materials choice, volume fractions and microstructure. Obvious prerequisites for use are that the membrane must be able to sustain a high oxygen flux and possesses a high stability under application conditions.

Previously, we employed the electrical conductivity relaxation (ECR) technique to measure the chemical diffusivity (D^{δ}) and the surface exchange coefficient (k^{δ}) of dual-phase composites $Sr_2Fe_{1.5}Mo_{0.5}O_{6-\delta}$ (SFM) - $Sm_{0.2}Ce_{0.8}O_{2-\delta}$ (SDC).[12] Whereas SDC is a well-known electrolyte showing promise for use in solid oxide fuel cells (SOFCs) operating at moderate temperatures,[13] the mixed-conducting double perovskite SFM has potential for use both as cathode and as anode because of its excellent chemical stability in oxidizing and reducing environments.[10,14-16] The results of ECR measurements in the range of oxygen partial pressure (pO_2) from 0.01 to 1 atm revealed that at all investigated phase volume fractions in the composite the relaxation process is entirely controlled by the surface exchange kinetics.[12] The addition of SDC to the SFM phase was found to significantly enhance the rate of oxygen incorporation. The results are interpreted to reflect the fast oxygen incorporation kinetics at the SFM-SDC-gas triple phase boundaries. Similar synergy has been observed for other mixed-conducting cathode materials by their impregnation or coating with oxide electrolyte nanoparticles.[17-19]

The present work builds on our previous study[12] by extending the ECR measurements on SFM-SDC dual-phase composites towards reducing atmospheres. Gas mixtures of H_2/H_2O and CO/CO_2 are used to control pO_2 steps in the range 10^{-24} - 10^{-20} atm. The observed oxygen release kinetics is correlated with the volume fractions of both constituent phases in the composites and the associated microstructure.

Experimental

Powder of SDC was prepared by the oxalate co-precipitation method using high purity cerium and samarium nitrates. Powder of SFM was synthesized by a microwave-assisted combustion method. Full details of both synthesis routes are described in our previous paper.[12] Both powders were mixed in appropriate proportions by ball milling in ethanol for 2 h. The volume fraction of the SDC phase in the powder mixtures varied between 0.105 and 0.667. The powder mixtures were uniaxially pressed (320 MPa), and sintered in air at 1350 °C for 5 h to obtain rectangular bars with dimensions of about 20 × 4.8 × 0.6 mm^3. Their density measured by the Archimedes method as well as the geometrical density was well above 96% of the theoretical one. The surface morphology of the sample bars was investigated by scanning electron microscopy (SEM, JSM-6700F). The length of the TPB and the surface area of both constituent phases in the composite were determined using Image-Plus software (Media Cybernetics Company). Images from at least five different areas of each sample were used to obtain average data.

For conductivity and ECR measurements, the sample was mounted in a quartz tube. Electrical connections to the sample were established by silver wires (ø = 0.10 mm). Silver paste (Sina-Platinum Metals Co., Ltd) was used to improve the contact between the bar specimen and the wires. Conductivity measurements were performed, at 750 °C, using the standard 4-probe dc technique. In ECR experiments, the conductivity was measured as a function of time following a step-wise decrease in the ambient pO_2, which was performed by switching the gas stream (a) from room-temperature (~ 3%) humidified 60:40 H_2/Ar ($pO_2 = 2.6 \times 10^{-23}$ atm) to humidified pure H_2 ($pO_2 = 9.4 \times 10^{-24}$ atm), and from (b) 1:1 CO/CO_2 ($pO_2 = 1.3 \times 10^{-20}$ atm) to 2:1 CO/CO_2 ($pO_2 = 3.4 \times 10^{-21}$ atm), at a flow rate of 200 ml min^{-1}. The flush time of the reactor was less than 1 s. Prior to the measurements, the samples were pre-equilibrated for 1 h in the gas stream used before gas switching. The experimental data were numerically fitted to eqns (1)-(3),

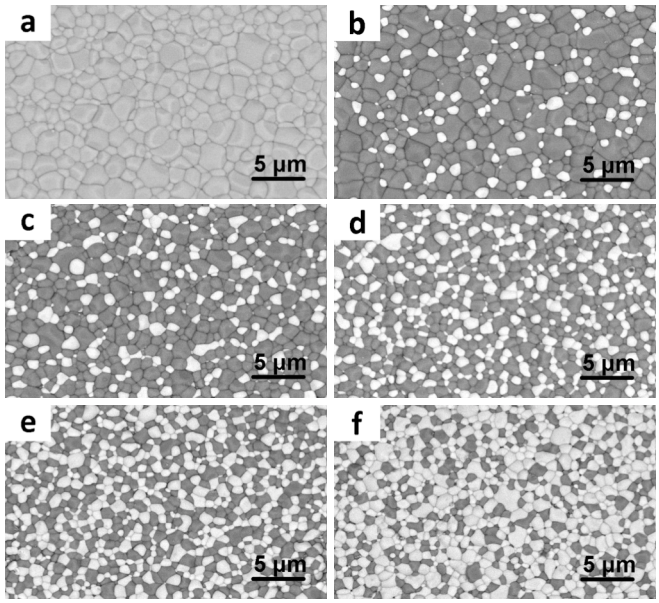

Fig. 1 SEM surface images of SFM–SDC composites with different SDC phase volume fractions: (a) 0, (b) 0.105, (c) 0.223, (d) 0.353, (e) 0.501, and (f) 0.667.

$$g(t)=\frac{\sigma(t)-\sigma_0}{\sigma_\infty-\sigma_0} = 1-\prod_{i=x,y,z}\sum_{m=1}^{\infty}\frac{2L_i^{\,2}}{\beta_{m,i}^{\,2}(\beta_{m,i}^{\,2}+L_i^{\,2}+L_i)}\cdot\exp(-\frac{t}{\tau_{m,i}}) \quad (1)$$

$$\tau_{m,i}=\frac{b_i^2}{D^{\delta}\beta_{m,i}^2} \quad (2)$$

$$L_i=\frac{b_i}{L_c}=\beta_{m,i}\tan\beta_{m,i} \quad (3)$$

where $g(t)$ is the normalized conductivity, σ_0 and σ_∞ are the conductivities, $\sigma(t)$, at time $t = 0$ and $t = \infty$, respectively, k^{δ} is the surface exchange coefficient, D^{δ} is the chemical diffusion coefficient, $2b_i$ is the sample dimension along coordinate i, $\beta_{m,i}$ are the non-zero roots of eqn (3), and $L_c = D^{\delta}/k^{\delta}$ is the critical length scale below which oxygen surface exchange becomes predominant over bulk oxygen diffusion in determining the rate of re-equilibration. Detailed descriptions of the ECR technique and the model used for data fitting are given elsewhere.[20]

Results and discussion

Microstructural investigations

Microstructural investigations of the SFM-SDC composites were conducted using SEM, image analysis, and X-Ray diffraction. Here, only the main findings are briefly recalled.

	k^{δ} [m s^{-1}] O_2 (N_2 balance) pO_2 step = 0.1 atm → 1 atm	k^{δ} [m s^{-1}] CO/CO_2 pO_2 step = 1.3×10^{-20} atm → 3.4×10^{-21} atm	k^{δ} [m s^{-1}] H_2/H_2O (Ar balance) pO_2 step = 2.6×10^{-23} atm → 9.4×10^{-24} atm
SFM	$(3.7 \pm 0.3) \times 10^{-7}$ [Ref. 12]	$(6.1 \pm 0.5) \times 10^{-7}$	$(2.3 \pm 0.3) \times 10^{-6}$
SDC	---	$(3.4 \pm 0.2) \times 10^{-7}$	$(1.6 \pm 0.1) \times 10^{-7}$

Table 1 Oxygen surface exchange coefficients k^{δ} of pure SDC and SFM measured at 750 °C in different gas environments. Data for SFM measured under oxidizing conditions (pO_2 step: 0.1 → 1 atm) from our previous work is given for comparison.[12] The quoted errors are estimated errors for k^{δ} obtained fitting of multiple conductivity transients for a given sample.

Surface SEM micrographs of the composites are shown in Fig. 1, showing that the grains of both constituent phases are homogeneously dispersed. The average grain size increases slightly from 1 μm to 1.7 μm for SDC, and decreases from 3 μm to 1 μm for SFM upon increasing the volume fraction of SDC in the composite from 0.105 to 0.667. Neither SEM, nor X-ray diffraction patterns of the composite powders or ceramics showed evidence of impurity phases. Image analysis of the SEM micrographs confirmed that a maximum in the TPB length occurs at a SDC phase volume fraction of 0.5, reaching a value of around 1.7×10^6 m per unit area (m^2). More detailed discussions on the microstructure of the composites under consideration are given in our previous paper.[12]

Electrical conductivity

Fig. 2 shows the electrical conductivity of SDC-SFM composites, at 750 °C, in reducing atmospheres as a function of the SDC phase volume fraction. SFM clearly is the constituent in the composite with the higher conductivity. Its conductivity in humidified 60% H_2/Ar ($pO_2 = 2.6 \times 10^{-23}$ atm) is 26 S cm^{-1}, which is comparable to values reported for the double perovskites $SrMgMoO_6$ and $SrMnMoO_6$.[21,22] The high degree of oxygen nonstoichiometry of SDC under these reducing conditions gives rise to predominant *n*-type conductivity. The measured conductivity of 0.4 S cm^{-1} is in agreement with literature data,[23] and is higher, by a factor of 4, than the reported ionic conductivity of SDC.[13] The electrical conductivities of SFM and SDC both increase upon lowering the pO_2 from 1.4×10^{-20} atm to 2.6×10^{-23} atm, as can be inferred from Fig. 2. Furthermore, the conductivity of the composite expectedly decreases with increasing the volume fraction of SDC. Many approaches have been used for evaluation of the electrical conductivity of two-phase composite systems, but such an analysis was considered beyond the scope of this work.

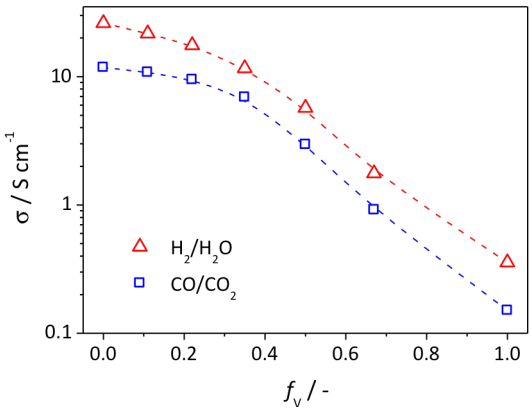

Fig. 2 Electrical conductivity σ of SFM–SDC composites as a function of SDC phase volume fraction f_V, at 750 °C, in different reducing atmospheres: humidified (~3%) 60:40 H_2/Ar ($pO_2 = 2.6 \times 10^{-23}$ atm) (*triangles*), and 1:1 CO/CO_2 ($pO_2 = 1.3 \times 10^{-20}$ atm) (*squares*). Lines are drawn to guide the eye.

Electrical conductivity relaxation

ECR measurements were carried out to study the oxygen release kinetics of SFM-SDC composites in reducing environments. Experimental data were acquired, at 750 °C, by switching between two H_2/H_2O (Ar balance), or CO/CO_2, gas streams with a different pO_2. Typical normalized conductivity transients measured in the two distinct atmospheres are shown in Fig. 3. Attempts to fit the relaxation data of both series to eqns 1-3, assuming mixed control of diffusion and surface exchange, yielded eigenvalues L_i significantly smaller than 0.03. The results indicate a re-equilibration that is predominantly controlled by the surface exchange kinetics.[20] Error plots of D^{δ} and k^{δ} obtained from fitting showed that for all curves the goodness-of-fit, by means of the minimum standard error of regression, is invariant to the value of D^{δ}. Values of k^{δ}

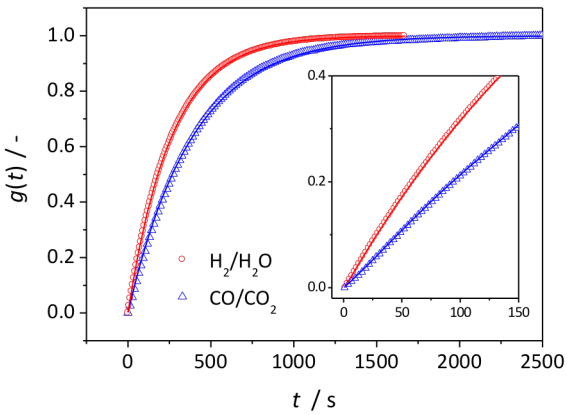

Fig. 3 Typical normalized conductivity transients for SFM-SDC composites after a step-wise decrease of pO_2 in H_2/H_2O (*circles*) and CO/CO_2 (*triangles*) atmospheres. The inset shows a magnification of both transients in the initial time period. The solid lines are the best fit of the experimental data to eqn 4. For clarity of presentation, the number of data points has been adapted in both figures. Data are shown for the composite with SDC phase volume fraction, $f_V = 0.353$.

for the pure SFM and SDC from fitting are listed in Table 1. Note that for SFM, k^{δ} is about 3 times larger under the more reducing conditions of the H_2/H_2O experiment than it is under CO/CO_2. For SDC, however, the opposite trend is observed, where it is found that k^{δ} is larger, by a factor of about 2, under CO/CO_2 atmosphere. A similar trend has been noted for k^{δ} of 10 mol% Gd-doped CeO_2 by Yashiro et al.[24] The results indicate that, in addition to the pO_2, the nature of the gaseous species determines the rate of the surface exchange reaction. Due to oxygen stoichiometry changes of both constituent phases during re-equilibration, as will be discussed below, k^{δ} cannot be defined for the composites. The normalized conductivity data of the composites were fitted by the exponential time dependence,

$$g(t) = 1 - \exp(-t/\tau_{\text{eff}}) \tag{4}$$

where τ_{eff} is the effective time constant. Eqn (4) is the reduced form of eqn (1) (with $\tau_{\text{eff}} = V/k^{\delta}S$, where V is the volume, and S is the geometrical surface area) when the relaxation process is under control of oxygen surface exchange alone.

As the electrical conductivity of the SFM phase predominates over that of SDC in the composites, it is primarily the change in oxygen stoichiometry of SFM that is probed by means of ECR. Under the reducing conditions covered by the experiments, SFM and SDC both release oxygen during re-equilibration of the composite with the lower pO_2 of the ambient after gas switching. It is tacitly assumed that oxygen transfer between SFM and SDC phases via internal surfaces (i.e., two phase boundaries) is fast relative to the oxygen exchange reactions occurring at their gas-exposed surfaces. This assumption is validated, albeit indirectly, by the observation of surface exchange-controlled relaxation kinetics (unless the two-phase boundaries would be entirely blocking for oxygen transfer). As a consequence, the relaxation process is determined by the rates of the oxygen exchange reaction at both SFM and SDC surfaces, and the degree to which both materials adapt their oxygen stoichiometry to attain equilibrium with the new pO_2.

Under the assumption of a diffusive equilibrium of ionic and electronic charge carriers within the composite, the differential mass balance equations for the constituent phases in the SFM-SDC composite read (wherein parameters of the SFM and SDC phase are designated with and without a prime, respectively),

$$f_V V \frac{\partial c(t)}{\partial t} = -f_S S k\,[c(t) - c(\infty)] + \frac{\partial n}{\partial t} \tag{5}$$

$$(1-f_V) V \frac{\partial c'(t)}{\partial t} = -(1-f_S) S k'\,[c'(t) - c'(\infty)] - S k'_{\text{syn}}\,[c'(t) - c'(\infty)] - \frac{\partial n}{\partial t} \tag{6}$$

where V is the total volume, S is the total geometrical surface area exposed to the gas phase, whilst f_V and f_S denote the volume and surface area fractions, respectively, k is the intrinsic surface exchange coefficient,[25] and $c(0)$ and $c(\infty)$ are the oxygen concentrations, $c(t)$, at time t = 0 and t = ∞, respectively. In conformity with our previous work,[12] we have added a contribution to eqn (6) that may arise from the enhancement of the exchange rate at the triple phase boundaries. The corresponding exchange coefficient, k'_{syn}, has been normalized on the total surface area, S (rather than, e.g., the length of the TPB). It is further noted that such a contribution, which is synergetic to the intrinsic exchange reactions at the SFM and SDC surfaces, could equally be added to eqn 5. We would then have a fourth possible exchange route via which release of oxygen occurs during re-equilibration with the gas phase. Assigning a single term to eqn (6) implies that the coefficient k'_{syn} is merely a lumped parameter. Oxygen concentration changes during the re-equilibration process are 'communicated' between both phases via the term $\partial n/\partial t$ in eqns (5) and (6), which denotes the rate of oxygen transfer via internal surfaces to maintain equilibrium.[26] Under the usual assumption of a linear relationship between electrical conductivity and oxygen concentration within the applied pO_2 step change, we have

$$g(t) = \bar{c}(t) = \frac{c(t) - c(0)}{c(\infty) - c(0)} \tag{7}$$

noting that $\bar{c}(t) = \bar{c}'(t)$. Eqns (5) and (6) can be solved into the form of eqn (4) with

$$\frac{1}{\tau_{\text{eff}}} = \frac{\alpha}{\tau} + \frac{(1-\alpha)}{\tau'} + \frac{(1-\alpha)}{\tau'_{\text{syn}}} \tag{8}$$

where

$$\frac{1}{\tau} = \frac{f_S S k}{f_V V}; \quad \frac{1}{\tau'} = \frac{(1-f_S) S k'}{(1-f_V) V}; \quad \frac{1}{\tau'_{\text{syn}}} = \frac{S k'_{\text{syn}}}{(1-f_V) V} \tag{9}$$

and

$$\alpha = \frac{f_V\big(c(\infty) - c(0)\big)}{f_V\big(c(\infty) - c(0)\big) + \big(1-f_V\big)\big(c'(\infty) - c'(0)\big)}$$
$$(1-\alpha) = \frac{\big(1-f_V\big)\big(c'(\infty) - c'(0)\big)}{f_V\big(c(\infty) - c(0)\big) + \big(1-f_V\big)\big(c'(\infty) - c'(0)\big)} \tag{10}$$

The latter two quantities denote the fraction of oxygen exchanged by SDC and SFM phases, respectively, relative to the total amount of oxygen exchanged between the composite and the gas phase. Surface exchange coefficients k and k' are evaluated from data of ECR measurements on the parent materials. Eqn (8) enables deconvolution of the observed time constant τ_{eff} in terms of τ, τ', and τ'_{syn} to analyse the contribution of the triple phase boundaries (k_{syn}) to oxygen surface exchange.

Fig. 4 shows values of τ_{eff} extracted from data of ECR measurements in the two different gas environments as a function of the phase volume fraction of SDC in the dual-phase composite. It should be noted that the value of $V/S \approx b$ (half-thickness) varied within about 4% for the different samples. Also plotted in Fig. 4 is τ_{calc}, which is the calculated time constant expected in the absence of a synergetic contribution to surface exchange: $1/\tau_{\text{calc}} = \alpha/\tau + (1-\alpha)/\tau'$. Values of α for a for a given pO_2 step change (see Experimental) were calculated

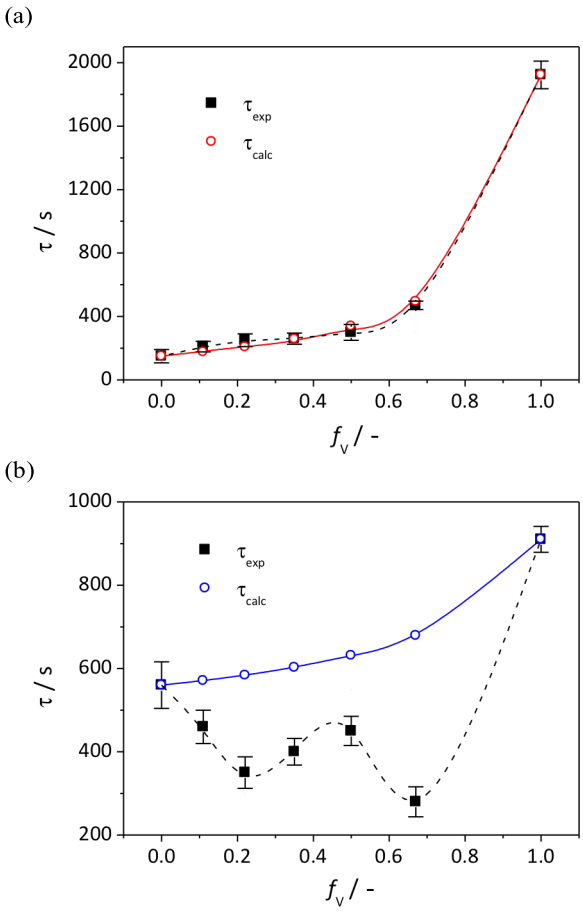

Fig. 4 Experimental (τ_{eff}) and calculated (τ_{calc}) time constants of conductivity relaxation as a function of SDC phase volume fraction f_V in: (a) H_2/H_2O and (b) CO/CO_2 atmospheres. Lines are drawn to guide the eye. Error bars represent the standard error with 95% confidence interval.

accord with eqn (10), using corresponding changes in the oxygen nonstoichiometry parameter δ of parent SDC and SFM. For SDC, $\Delta\delta = 0.0199$ and $\Delta\delta = 0.0060$ for the applied pO_2 step change under H_2/H_2O and CO/CO_2 atmospheres, respectively. By the lack of published data of the oxygen nonstoichiometry of SDC, these values were evaluated from thermogravimetric data of related 10 mol% Gd-doped CeO_2.[27] For SFM, for both pO_2 steps $\Delta\delta = 0.032$, which values were calculated using thermodynamic parameters derived from data of oxygen coulometric titration.[28] Fig. 4a shows that for the pO_2 step change under H_2/H_2O atmosphere, τ_{eff} almost coincides with τ_{calc}, indicating a negligible contribution of the SFM-SDC heterogeneous interfaces to the oxygen release kinetics. Accordingly, the relaxation response is a weighted average of the intrinsic contributions of both constituent phases in the composite. Different results are obtained for the pO_2 step change under CO/CO_2 atmosphere (Fig 4b), where it is found that $\tau_{eff} < \tau_{calc}$, suggesting a synergistic contribution to the oxygen surface exchange kinetics.

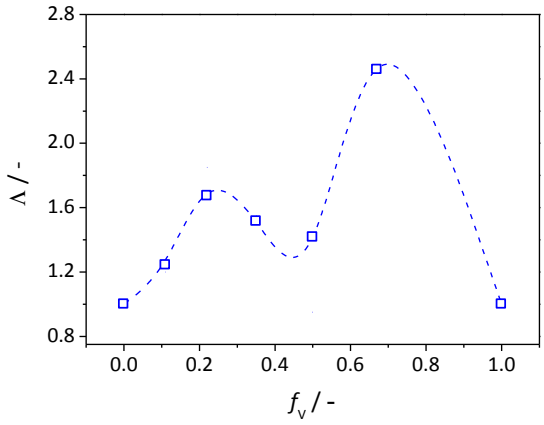

Fig. 5 Exchange rate enhancement factor Λ as a function of SDC phase volume fraction f_V in CO/CO_2 atmospheres. The parameter Λ is defined by eqn (12). Lines are drawn to guide the eye.

The oxygen flux, $\Re(t)$ [mol cm^{-2} s^{-1}], during re-equilibration is a function of time. Using eqns (4) and (7), it can be expressed as

$$\Re(t) = \frac{1}{S}\frac{\partial m}{\partial t} = \frac{1}{S}\frac{\partial \bar{c}(t)}{\partial t}\cdot m_{tot} = \Re_0 \cdot \exp(-t/\tau_{eff}) \quad (11)$$

where $\Re_0 = m_{tot}/S\tau_{eff}$, and m_{tot} is the total amount of oxygen exchanged between the composite and the gas phase once equilibrium is achieved. An enhancement factor, Λ, can be defined,

$$\Lambda = \left.\frac{\tau_{eff}}{\tau_{calc}}\right|_{t=0} \quad (12)$$

whose ratio expresses the measured oxygen exchange rate, at t = 0, relative to the calculated rate in the absence of the synergistic contribution (k'_{syn}). Corresponding data for the pO_2 step change in CO/CO_2 atmosphere are presented in Fig. 5. A maximum value for Λ of 2.4 is observed for the composite with SDC volume fraction f_V = 0.667. This value is notably smaller than the corresponding value derived from data of ECR measurements under oxidizing conditions (pO_2 range 0.01 – 1 atm). Under the latter conditions, the addition of SDC to SFM was found to enhance the rate of oxygen incorporation up to a factor of ~17.[12] The much lower, or even negligible (under H_2/H_2O atmosphere), enhancement of the oxygen release kinetics is attributed to the fact that both constituents SFM and SDC exhibit appreciable levels of mixed ionic-electronic conductivity under the reducing conditions covered by the experiments, diminishing the contribution of the TPB on overall exchange kinetics. This is in contrast with the situation under oxidizing conditions (oxygen incorporation), where mixed conductivity is mainly limited to the SFM phase, and the oxygen reduction kinetics is significantly enhanced by the addition of the electrolyte SDC. In this respect, one may anote that, for example, in the composite $(La,Sr)MnO_3$ (LSM) - yttria-stabilized zirconia (YSZ) cathode, where electronic and ionic conductivities are confined (to a great extent) to separate

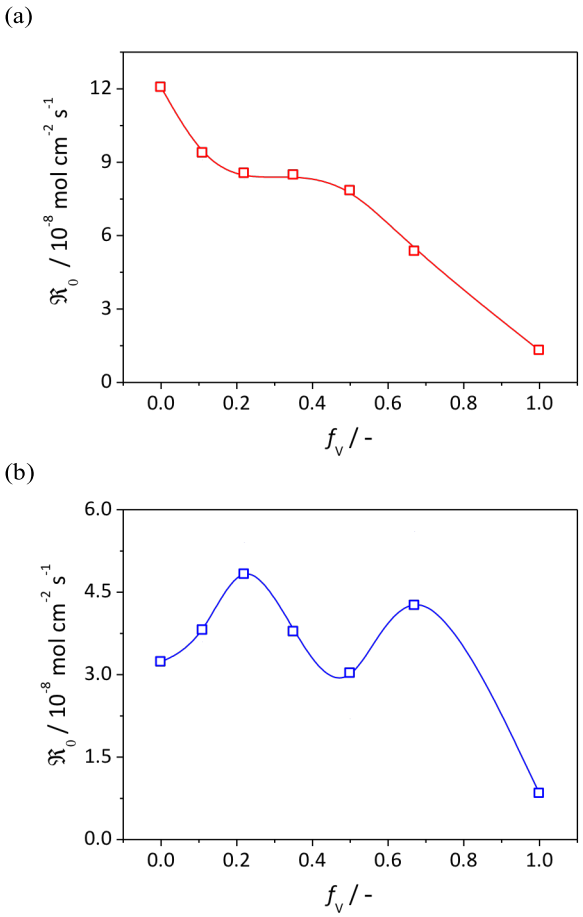

Fig. 6 Exchange rate $\Re_0$ as a function of the SDC phase volume fraction f_V from data of measurements under (a) H_2/H_2O and (b) CO/CO_2.

phases, the oxygen exchange reaction takes place almost exclusively at the TPB.[29,30] In Fig. 6, the rate parameter $\Re_0$ derived from data of ECR measurements under H_2/H_2O and under CO/CO_2 atmospheres is plotted as function of the SDC phase volume fraction in the composite. It can be inferred from this Fig. that the fastest oxygen release kinetics under conditions of H_2 oxidation is observed for pure SFM, whilst the fastest kinetics under conditions of CO oxidation is found for the composite with $f_V = 0.223$.

Fig. 7 shows a plot of k'_{syn} derived from data of ECR measurements under CO/CO_2 atmosphere versus the length of the TPB obtained from image analysis of the SEM surface micrographs (Fig. 1). It is immediately clear that no correlation emerges between both parameters, and additional factors must account for the observed behaviour. As already noted, the surface exchange rate is highly dependent on the nature of the gaseous species. Assuming, for example, a Mars-van Krevelen mechanism[31] for the oxidation of CO, the number density of preferentially adsorbed CO molecules may enter the rate limiting step. Although it is clear from the results of this study that heterogeneity may contribute to enhancement of the oxygen surface exchange kinetics, more work needs to be done to understand the role of the individual components within the composite.

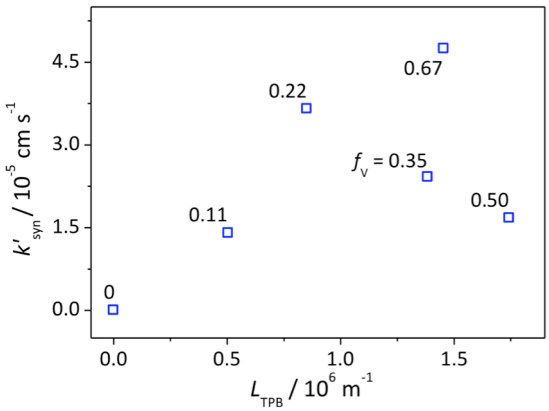

Fig. 7 Exchange coefficient k'_{syn} under CO/CO_2 atmosphere versus the length of the TPB (L_{TPB}) obtained from image analysis of the SEM surface micrographs (Fig. 1). Numbers shown at the data points denote the corresponding SDC phase volume fractions f_V.

Conclusions

At given thickness of the samples (~0.6 mm), the oxygen release kinetics of SFM-SDC composites under H_2/H_2O and CO/CO_2 atmospheres is controlled by the surface exchange kinetics. Whilst the effective time constant for equilibration of samples to the ambient pO_2 under H_2/H_2O atmosphere is determined by a weighted contribution of the surface exchange reactions occurring on the gas-exposed surfaces of both components in the composite, an enhanced exchange rate relative to the intrinsic contributions of the components is found when the ECR experiments are carried out under CO/CO_2 atmosphere. The enhanced exchange rate is attributed to synergetic effects caused by the heterogeneous interfaces.

The results of this and our previous study[12] confirm that the triple phase boundaries in SFM-SDC composites significantly accelerate the oxygen incorporation kinetics under oxidizing conditions, but only modestly, or even negligibly, influence the oxygen release kinetics under reducing conditions.

Acknowledgements

We gratefully acknowledge the financial support from the Ministry of Science and Technology of China (2012CB215403).

Notes and references

[a] *CAS Key Laboratory of Materials for Energy Conversion, Department of Materials Science and Engineering, University of Science and Technology of China, Hefei, 230026, P. R. China.*

[b] *Department of Science & Technology, MESA+ Institute for Nanotechnology, University of Twente, P.O. Box 217, 7500 AE Enschede, The Netherlands.*

1 Q. Jiang, S. Faraji, D. A. Slade and S. M. Stagg-Williams, in *Inorganic Polymeric and Composite Membranes - Structure, Function and Other Correlations*, Elsevier, 2011, vol. 14, pp. 235–273.

2 J. Sunarso, S. Baumann, J. M. Serra, W. A. Meulenberg, S. Liu, Y. S. Lin and J. C. Diniz da Costa, *J. Membrane Sci.*, 2008, **320**, 13–41.

3 M. A. Habib, H. M. Badr, S. F. Ahmed, R. Ben Mansour, K. Mezghani, S. Imashuku, G. J. la O, Y. Shao-Horn, N. D. Mancini, A. Mitsos, P. Kirchen and A. F. Ghoneim, *Int. J. Energ. Res.*, 2011, **35**, 741–764.

4 X. Dong and W. Jin, *Curr. Opin. Chem. Eng.*, 2012, **1**, 163–170.
5 M. Czyperek, P. Zapp, H. J. M. Bouwmeester, M. Modigell, K. Ebert, I. Voigt, W. A. Meulenberg, L. Singheiser and D. Stoever, *J. Membrane Sci.*, 2010, **359**, 149–159.
6 X. Zhu, Q. Li, Y. He, Y. Cong and W. Yang, *J. Membrane Sci.*, 2010, **360**, 454–460.
7 H.J.M. Bouwmeester, *Catal. Today*, 2003, **82**, 141–150.
8 M. P. Lobera, S. Escolástico, J. Garcia Fayos and J. M. Serra, *Chemsuschem*, 2012, **5**, 1587–1596.
9 O. Czuprat, S. Werth, J. Caro and T. Schiestel, *AICHE*, 2010, **56**, 2390–2396.
10 G. Xiao and F. Chen, *Fuel Cells*, 2014, **2**.
11 A. B. Stambouli and E. Traversa, *Renew. Sust. Energ. Rev.*, 2002, **6**, 433–455.
12 Y. Wang, B. Hu, Z. Zhu, H. J. M. Bouwmeester and C. Xia, *J. Mater. Chem., A*, 2014, **2**, 136–143.
13 M. Mogensen, N. M. Sammes and G. A. Tompsett, *Solid State Ionics,* 2000, **129**, 63–94.
14 G. Xiao, Q. Liu, S. Nuansaeng and F. Chen, *ECS Transactions*, 2012, **45**, 355–362.
15 G. Xiao, Q. Liu, F. Zhao, L. Zhang, C. Xia and F. Chen, *J. Electrochem. Soc.*, 2011, **158**, B455.
16 Q. Liu, X. Dong, G. Xiao, F. Zhao and F. Chen, *Adv. Mater. Weinheim*, 2010, **22**, 5478–5482.
17 L. Zhang, Y. LIU, Y. Zhang, G. Xiao, F. Chen and C. Xia, *Electrochem. Commun.*, 2011, **13**, 711–713.
18 Y. Wang and C. Xia, *J. Electrochem. Soc.*, 2012, **159**, F570–F576.
19 J. M. Vohs and R. J. Gorte, *Adv. Mater. Weinheim*, 2009, **21**, 943–956.
20 M. den Otter, H.J.M. Bouwmeester, B.A. Boukamp and H. Verweij, *J Electrochem. Soc.*, 2001, **148**, J1–J6.
21 Y. H. Huang, R. I. Dass, Z. L. Xing and J. B. Goodenough, *Science*, 2006, **312**, 254–257.
22 Y. H. Huang, R. I. Dass, J. C. Denyszyn and J. B. Goodenough, *J. Electrochem. Soc*., 2006, **153**, A1266–A1272.
23 J. Wright and A. V. Virkar, *J. Power Sources*, 2011, **196**, 6118–6124.
24 K. Yashiro, S. Onuma, A. Kaimai, Y. Nigara, T. Kawada, J. Mizusaki, K. Kawamura, T. Horita and H. Yokokawa, *Solid State Ionics,* 2002, **152**, 469–476.
25 Although the superscript δ has been omitted in the notation of the intrinsic surface exchange coefficients, k and k', one should keep in mind that both quantities represent 'chemical' values.
26 The situation resembles that of two water reservoirs connected to each other through a hose, and acting according to the principle of communicating vessels. If leaks are present in the bottom of the reservoirs, the leak rates will be determined by the temporary height ($h(t)$-$h(\infty)$) of the water column in the reservoirs. Transfer of water occurs between the reservoirs, and well to the one with the higher leak rate to level out the water levels in the two reservoirs.
27 S. Wang, H. Inaba, H. Tagawa, M. Dokiya and T. Hashimoto, *Solid State Ionics,* 1998, **107**, 73–79.
28 O.V. Merkulov, E.N. Naumovich, M.V. Patrakeev, A.A. Markov, H.J.M. Bouwmeester, A. Leonidov, and V.L. Kozhevnikov, *to be published*.
29 Y. Ji, J. Kilner and M. Carolan, *Solid State Ionics,* 2005, **176**, 937–943.
30 M. Backhaus-Ricoult, *Solid State Ionics,* 2006, **177**, 2195–2200.
31 P. Mars and D. W. Van Krevelen, *Chem. Eng. Sci.*, 1954, **3**, 41–59.

Graphical abstract